Influence of coaxial cables resistance on impedance measurements at low frequency and guidelines for phase determination of a.c. electrical signals

Boris Chenaud, Carlos Hernández, Adrien Delgard, Christophe Chaubet

Influence of coaxial cables resistance on impedance measurements at low frequency and guidelines for phase determination of a.c. electrical signals

Boris Chenaud,[1] Carlos Hernández,[2] Adrien Delgard,[1] and Christophe Chaubet*[1]
[1)] *L2C, Univ Montpellier, CNRS, Montpellier, 34095, France*
[2)] *Departamento de Física, Universidad Militar Nueva Granada, Carrera 11 # 101-80, Bogotá D.C., Colombia*

(*Electronic mail: christophe.chaubet@umontpellier.fr)

(Dated: 6 November 2023)

We present an experimental study on a.c. measurements at low frequency (below 1MHz), when coaxial cables used for the measurement are resistive, as in cryogenic conditions. More precisely we are interested in admittance or impedance measurements and the accurate determination of the phase. Our experiments were completed using an auto-balancing bridge impedance analyzer and various standard coaxial cables as well as their serial combinations. We characterize experimental setup, then we analyze and measure the phase shift introduced in impedance measurements by leads resistance. Using basic equations for electrical signal propagation in coaxial cables, we calculate phase shift in the whole frequency range and explain our data in the low frequency limit of our model. We propose a quantitative criterion to determine whether the experimental context is appropriate. If not, we show that by using an original calibration procedure the imaginary part can be accurately recovered, avoiding artifacts. The calibration procedure can be applied to any a.c. voltage or current measurement, whatever the detection technique, with known accuracy.

I. INTRODUCTION

Understanding the response of an electrical circuit to an alternating excitation requires first to measure currents and voltages. The purpose in this article is to illustrate experimentally how those quantities are influenced by the lead resistance of the cables at low frequency (below 1MHz). We consider here the example of impedance and admittance measurement, which requires to measure simultaneously current and voltage, whose ratio delivers the linear response of the circuit. More precisely we focus on the imaginary part of the signal and all corrections that might hinder the phase determination. We detail the procedure for accurate measurements. Our conclusions, deduced from impedance or admittance measurements, apply in fact to any a.c. electrical measurements.

Impedance measurement is a well known technique for characterization of electrical properties at finite frequency[1] with many applications ranging from electronics to life sciences[2,3]. Nowadays, impedance analyzers are easy to operate and allow a fast measurement procedure with high repeatability[4–6], although their accuracy drops at very low frequencies (below 10 kHz see Ref.[6]).

For decades, metrologists working on the Ohm's conservation have been concerned with side effects of coaxial cable[7–9] and with intrinsic inductances and capacitances[10], in order to reduce the deviations of Hall resistance measurements from the quantized value, at low frequency[11–13]. They have been mainly concerned with the real part of the impedance (the Hall resistance) although some works have explored the imaginary part[14–16]. They finally built the double shielded device[17,18], a resistance standard in which the real part do not depend anymore on frequency.

Even when metrological accuracy is not needed, a detailed analysis of the experimental setup is necessary to avoid systematic errors[19] and take into account the effects of cables[20]. In general, main corrections in a.c. voltage measurement arises from the capacitance C and the inductance L of the coaxial cable, but not from the cable resistance, which is usually negligible.

As a striking example of cable capacitance influence on impedance measurement, Melcher et al. explained in Ref.[21], how the cables have blurred the measurement (at kHz frequencies) of small quantum capacitances in Ref.[22]. Later, C. Hernández et al.[23,24] used the principle of current loss in cable capacitance explained by Fisher and Grayson[25], to obtain the admittance of multi-terminal quantum Hall conductors by a combined effect of chiral currents and cable capacitance. They showed that any coaxial cables connected to an ohmic contact on the high potential side of the Hall bar, introduces a phase shift $\varphi = R_{\mathrm{H}} C_{\mathrm{cable}} \omega$ in the admittance measurement, where C_{cable} is the cable capacitance and R_{H} the Hall resistance. This phase shift prevents the small intrinsic imaginary part (related to quantum capacitance) to be precisely measured. However, the influence of a coaxial cable on the phase does not rely only on its capacitance: it relies also on its resistance, even small.

In an Helium cryostat or in a dilution fridge, one or two meters cables are usually needed to access low temperatures stage. To reduce the thermal power input when working below liquid Helium temperature, resistive cables (thermally and therefore electrically) are chosen most of the time. For a description of a full controlled environment for metrological measurements at cryogenic temperatures, see Refs.[26,27].

In this article, we experimentally highlight the resulting artefact which appears in the imaginary part of the measured impedance, when resistive cable ($R \geq 1\Omega$) are used to connect the sample to the a.c. bridge, at low frequencies. This effect was first described theoretically in Ref.[28] and Ref.[29], in the approximation of quasi stationary regime (AQSR). Here we focus on the experimental consequence which results in a phase shift in the impedance or admittance measurements. This phase shift is proportional to the resistance and to the ca-

pacitance of the cable ($\varphi = R_{\rm cable}C_{\rm cable}\omega$). Of course, for short and standard cables this shift is not observable. Contrarily, in the case of resistive cables of some meters long ($R \geq 1\Omega$), like in cryogenic environment, the phase shift is enough to blur measurements of μH inductances such as encountered in quantum electronics. In recent years indeed, quantum inductances were unveiled in nano-inductors[30–32], quantum coherent circuit[33,34] or plasmons devices[35–38]. Those studies were performed at very high frequencies using GHz techniques, which are totally different from those presented here. However, measurement of those inductances might also be done at low frequency[39,40], taking into account the cables influence. In this article, we give the calibration procedure to get rid of the artefact induced by the lead resistance.

It is important to notice that the artefact would arise in fact in any experimental situation where an a.c. voltage or an a.c. current is measured using resistive coaxial cables, in link with a physical quantity, not only the impedance. This includes of course standard lock-in amplifier detection techniques. However, many publications involving a.c. measurements under cryogenic conditions, do not mention which cables are used neither their resistance, although measurements need a fine analysis of the imaginary part to precisely explore the phase. Refs.[41–43] are examples where physical quantities are measured through an a.c. voltage in cryogenic conditions, concerning respectively, magnetic susceptibilty, calorimetry and low field NMR. In absence of cable specifications, the phase is possibly affected by the lead resistance, exactly as for the impedance here.

The paper is organized as follows: in section II, we present a basic experiment at low frequency which highlights how the lead resistance blurs the imaginary part of the impedance. In section III, we use the model of wave propagation in a coaxial cable to obtain the phase shift in the whole frequency range. In section IV we detail the calibration experiment and we show how to get rid of the artefact. We present further experimental results on several series combinations of cables, to highlight features that are important for accurate measurements. In the following, we denote by f the frequency (always below 1MHz in our experiments), and $\omega = 2\pi f$ is the angular frequency.

II. A BASIC EXPERIMENT INVOLVING RESISTIVE COAXIAL CABLES

To highlight role of coaxial cables resistance in an admittance measurement, we present in Fig.1 the result of a very simple experiment, which will be analyzed in detail in section IV to characterize the cable set. We have measured in two different ways the admittance of a metallic resistor, known to have a vanishing susceptance. All measurements are done at $T = 300\,$K with an impedance analyzer "Agilent 4294A", and are fully described in section III. In a first experiment, we measured the susceptance of a metallic resistor placed directly on the impedance analyzer, without cables, using a component adaptor (see green triangles on Fig.1). Those metallic resistors are thin metallic films deposited on a ceramic and have very small inductances and capacitances (usually $\leq 0.1\,\mu$H and $\leq 0.1\,$pF respectively). For those resistors, we could not measure any inductance and we found a stray capacitance of 0.15 pF (green curve Fig. 1).

In a second experiment, the metallic resistor was placed at the end of 6 meters cables of total resistance $64\,\Omega$; we made same measurements for two resistors, $12\,$kΩ and $24\,$kΩ (red squares in Fig.1). We present here only the imaginary part of the admittance, given that the resistor conductance (real part of admittance) does not vary in this frequency range. It is not shown here but behavior of conductances is exactly the same with and without long cables (the effect of cables on the conductance measurement is too small to be measured in our experiment, as detailed in section III.D). However, it goes differently for the imaginary part of admittance: it is clear on Fig.1 that the susceptance obtained using cables are very different from the true susceptance of the resistor, which is nearly zero. The red curves indicate undoubtly an artefact, which is clearly proportional to conductance of the resistor.

The artefact is due to the influence of lead resistance on

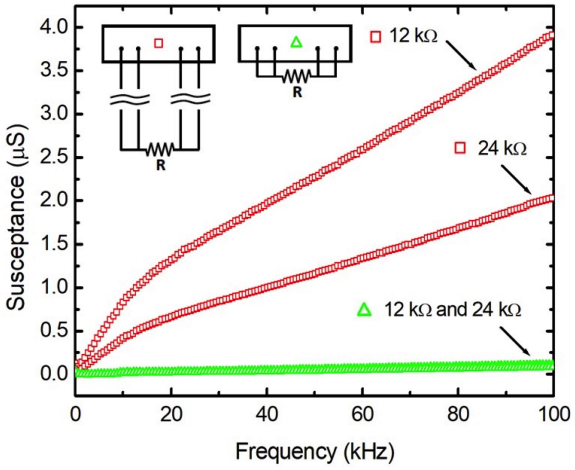

FIG. 1. Imaginary part of admittance for two metallic resistances, as function of frequency. Red squares: resistors are placed at the end of long resistive cables. Green triangles: resistors are placed directly on the impedance analyzer adaptor. $T = 300\,$K.

admittance measurement. The effect of cable resistance has been explained long ago by Cutkosky[28], detailed in Ref.[29] but theoretically and not experimentally, and only mentioned in Ref.[14,15]: when measuring an admittance Y in a four terminal-pair in AQSR with four identical resistive cables, the experiment gives

$$Y_{\rm exp} = Y(1+yz)\,. \qquad (1)$$

Here y and z are the impedance and conductance of a single cable, namely $y = jC_{\rm cable}\omega$ and $z = R_{\rm cable} + jL_{\rm cable}\omega$, such that in the AQSR regime:

$$Y_{\rm exp} = Y(1 + jR_{\rm cable}C_{\rm cable}\omega)\,. \qquad (2)$$

Cable capacitance and resistance thus add an extra term (proportional to real part of Y) to the imaginary part of the admittance. As the true susceptance is nearly vanishing here,

red curves in Fig.1 correspond exactly to the extra term. We will return on this experiment in section IV to calibrate the cable set by measuring the characteristic time $\tau_c = R_{\text{cable}} C_{\text{cable}}$, and get rid of the artefact. In this article, we thus exhibit experimental consequence of lead resistance effect described in Ref.[29], which consists in a phase shift $\varphi = \omega \tau_c$ in the admittance measurement.

III. MEASURING IMPEDANCES WITH RESISTIVE CABLES

In this section, we first recall the measuring principle of an auto-balancing a.c. bridge. Then we use the standard model of electrical signal propagation in coaxial cables to calculate the corrections introduced by the lead resistance for all frequencies, not limited to AQSR. We obtain the results of Ref.[29] as the low frequency development of a more general formula.

A. Principle of measurement for auto-balancing a.c. bridge

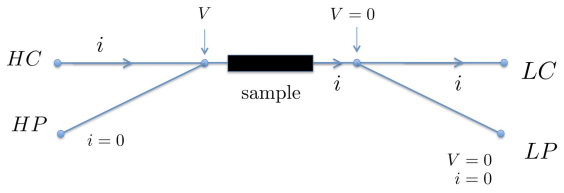

FIG. 2. Simplified guidelines for impedance measurement according to standard definition of impedance, and used by impedance analyzer "Agilent 4294A"[44]. Shielding is not represented here.

The convention for impedance measurements has been defined by metrologists (see for example Refs.[29,44,45]) and is depicted in figure 2. We use 4 coaxial cables to connect the sample to the impedance analyzer. In a four terminal-pair configuration, the auto-balancing a.c. bridge applies the following protocol: LP (Low Potential) terminal-pair is maintained at $V = 0$ and $i = 0$ without being connected to the ground (it is a virtual ground). The other side of the sample is connected to the HC (High Current) terminal-pair which injects a current by applying a finite potential $V \neq 0$. The potential is measured using the HP connector (High Potential). At the level of connector LC (Low Current), the auto-balancing bridge delivers a current in opposition with the current i in the sample. To do so, the impedance analyzer sets a potential V_R through a polarization resistor R_r, and the potential V_R is chosen in order to maintain $i = 0$ and $V = 0$ on the LP terminal-pair (see Ref.[44]), so that $V_R = R_r i$.

Under these conditions impedance analyzer measures V_{HP} and V_R; it then performs the operation

$$Z = R_r \frac{V_{HP}}{V_R} = \frac{V}{i} \,. \tag{3}$$

B. Measuring voltage and current using a resistive cable

The two fundamental characteristics of the coaxial cable "a" are its impedance Z_a and its propagation coefficient γ_a given by the relations[46,47]:

$$Z_a = \sqrt{\frac{R_a + jL_a\omega}{G_a + jC_a\omega}}, \tag{4}$$

$$\gamma_a(\omega) = \sqrt{(R_a + jL_a\omega)(G_a + jC_a\omega)}, \tag{5}$$

where R_a, L_a, C_a and G_a are respectively the resistance, the inductance, the capacitance and the dielectric conductance of the coaxial cable. Importantly, the resistance R_a of the cable "a" is the sum of the resistances of the outer and inner conductors. The dielectric conductance G_a between inner and outer conductor is sufficiently small to assume that $G_a = 0$ in the following (it might be different at higher frequencies).

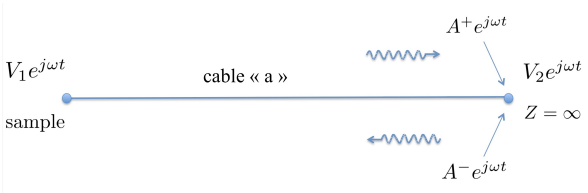

FIG. 3. Coaxial cable "a" (R_a, C_a) is used to measure potential V_1 using a voltmeter of infinite input impedance. Voltmeter measures potential V_2, not in phase with V_1 if cable resistance is finite.

A coaxial cable with parameters Z_a and γ_a is used to measure potential $V_1 e^{j\omega t}$ at sample side (see Fig.3). The voltmeter (infinite input impedance) measures $V_2 e^{j\omega t}$ at the other end of the coaxial cable. The usual model for propagation in coaxial cables[47] considers two counter propagating potential waves: A^+ and A^- are the complex amplitudes of these two waves at right end. The currents and the potentials on both end are obtained using continuity relations:

$$i_2 = \frac{A^+ - A^-}{Z_a} = 0, \tag{6}$$

$$V_2 = A^+ + A^-, \tag{7}$$

$$V_1 = A^+ e^{\gamma_a} + A^- e^{-\gamma_a}. \tag{8}$$

We obtain the relation between V_1 and V_2:

$$V_1 = V_2 \cosh(\gamma_a) \,. \tag{9}$$

The ideal case of a perfect cable, $R_a = 0$, would result in a pure propagative coefficient $\gamma_a = j\omega\tau_t$ where $\tau_t = \sqrt{L_a C_a}$ is the transit time of the wave along the cable. Eq.(9) would become $V_1 = V_2 \cos(\omega\tau_t)$, which shows that a perfect cable does not introduce any phase shift between V_1 and V_2, but modifies the voltage amplitude: resonances occur for $\omega\tau_t = (k+1/2)\pi$ ($f \approx 50\,\text{MHz}$ for a 1 m cable and $k = 0$).
However, when using resistive cables $\gamma_a = \sqrt{jR_aC_a\omega - \tau_t^2\omega^2}$.

Thus, even in the AQSR where $\tau_t^2\omega^2 \ll 1$, a phase shift appear between V_1 and V_2. This phase shift depends on both the capacitance and the resistance of the cable. As the capacitance of coaxial cables does not vary much from one cable to another (always more or less around 100 pF/m), the relevant characteristic here is the cable resistance, which varies in a large range depending on the alloy and section of the inner and outer conductors.

The same calculation for the current, depicted in Fig.4, gives the following expression for the current i_2:

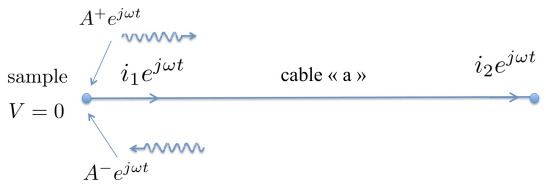

FIG. 4. Potential on sample side is maintained at $V = 0$ by the a.c. bridge using a cable connected to LP. A current i_1 flows through the sample. At right end, i_2 is measured.

$$i_2 = i_1 \cosh(\gamma_a) \, . \tag{10}$$

C. Impedance measurement using 4 resistive cables

We now consider the measurement of an impedance using a set of four long and resistive cables to connect comfortably the sample to sockets HP, LC, HC and LP of impedance analyzer. As seen above, the cables connected to HP and LC influence the measurement. Extending cables connected to LP and HC has no effect, as yet mentioned in Ref.[29]. Indeed, the cable connected to the LP terminal-pair is characterized by $V = 0$ and $i = 0$ at all time and everywhere on the cable, whatever its length. Besides, the cable connected to HC is used to inject current and its length has no effect either. Using Eq.(9) and Eq.(10), the impedance-meter finally measures both potentials:

$$V_{\rm HP} = V/\cosh(\gamma_a), \tag{11}$$
$$V_{\rm R} = R_{\rm r} i \times \cosh(\gamma_a), \tag{12}$$

where V and i are the potential and current experienced by the sample. Using Eq.(3) impedance analyzer returns the value

$$Z_{\rm exp} = R_{\rm r}\frac{V_{\rm HP}}{V_{\rm R}} = \frac{V}{i} \times \frac{1}{\cosh^2(\gamma_a)} \, . \tag{13}$$

We finally obtain the relation between the experimental impedance $Z_{\rm exp}$, and the true value Z of the impedance:

$$Z_{\rm exp} = \frac{Z}{\cosh^2(\gamma_a)} \, , \tag{14}$$

$$\text{with } \gamma_a = \sqrt{j\tau_a\omega - \tau_t^2\omega^2} \, . \tag{15}$$

The time $\tau_a = R_aC_a$ acts as a "delay" introduced by the set of four cables "a", more precisely by only two of them: the cable connected to HP and the cable connected to LC. The admittance obeys a symmetrical equation,

$$Y_{\rm exp} = Y\cosh^2(\gamma_a) \, . \tag{16}$$

D. Low frequency development

The above formula is valid at any frequency provided that the radio-electric model of wave propagation holds. Particularly, low frequency development of Eq.(15) gives

$$\cosh^2(\gamma_a) \approx 1 + \gamma_a^2 \approx (1 - L_aC_a\omega^2) + jR_aC_a\omega \, . \tag{17}$$

Consequently, measuring with resistive cables a dipole (G,C) of admittance $Y = G + jC\omega$, yields from Eq.16:

$$Y_{\rm exp} = G(1 - L_aC_a\omega^2) - C\tau_a\omega^2 + j(C + G\tau_a)\omega, \tag{18}$$

where $\tau_a = R_aC_a$. The cable resistance appears in both the real part and the imaginary part. Another quadratic term $(-C\tau_a\omega^2)$, generally much lower than $L_aC_a\omega^2$ except in particular conditions, is added to the real part. At 100kHz, $L_aC_a\omega^2 \approx 10^{-4}$ is not measurable by our means, so that in AQSR, $\cosh^2(\gamma_a) \approx 1 + jR_aC_a\omega$, and Eq.18 reduces to:

$$Y_{\rm exp} = Ye^{j\omega\tau_a} = G + j(C + G\tau_a)\omega, \tag{19}$$
$$\tau_a = R_aC_a \, . \tag{20}$$

At low frequency then, corrections introduced by cables result in a phase shift, which adds an extra term $G\tau_a\omega$ to the imaginary part, but only if the conductance is finite. The regime $G = 0$ is therefore indicated to make a direct measure of quantum capacitances[39,48,49]. In the general case $G \neq 0$, and to obtain the true value B of the susceptance, it is necessary to subtract $G\tau_a\omega$ from the measured imaginary part. In other words, it is necessary to subtract $G\tau_a$ from the measured capacitance to obtain C.

In the (R,X) mode of the impedance-analyzer, measurements of an impedance $Z = R + jL\omega$ using resistive cables "a" gives:

$$Z_{\rm exp} = R(1 - L_aC_a\omega^2) - L\tau_a\omega^2 + j(L - R\tau_a)\omega, \tag{21}$$

which becomes, in the AQSR

$$Z_{\rm exp} = Ze^{-j\omega\tau_a} = R + j(L - R\tau_a)\omega \, , \tag{22}$$

Again the phase is shifted, which adds an extra term $(-R\tau_a\omega)$ to the imaginary part, if the resistance is finite. Reactance X is always correctly measured if $R = 0$: in Ref.[40], Delgard et al. made a direct measurement of quantum inductances of Hall bars, taking profit of the zero-resistance state of the quantum Hall effect. In the general case $R \neq 0$, one must add $R\tau_a$ to the measured inductance, to obtain L.

E. Result for a two cables series

Most of the time, cables used for wiring inside the cryostat are different from standard coaxial cables used outside the cryostat to connect instruments. If cables "a" are inside the cryostat and are connected in series with cables "b" which are outside the cryostat, the impedance measurement using 4 serial cables "a" and "b", gives the result (see appendix)

$$Y_{\rm exp} = Y\left(\cosh(\gamma_{\rm a})\cosh(\gamma_{\rm b}) + (Z_{\rm a}/Z_{\rm b})\sinh(\gamma_{\rm a})\sinh(\gamma_{\rm b})\right)^2 . \tag{23}$$

The low frequency development of this formula gives the result obtained in Ref.[50] for two cables in AQSR:

$$Y_{\rm exp} = Ye^{j\omega\tau_c}, \tag{24}$$

$$\tau_c = R_{\rm a}C_{\rm a} + R_{\rm b}C_{\rm b} + 2R_{\rm a}C_{\rm b} . \tag{25}$$

Symetrically, measuring an impedance would lead to:

$$Z_{\rm exp} = Ze^{-j\omega\tau_c} . \tag{26}$$

For two identical cables "a = b", this formula yields $\tau_{\rm c} = 4R_{\rm a}C_{\rm a} = (2R_{\rm a}) \times (2C_{\rm a})$, showing that Eq.(25) is compatible with Eq.(20) for a single cable with double length. This equation shows that even if cable "b" outside the cryostat has no resistance ($R_{\rm b} = 0$), it enhances anyway the time delay: $\tau_{\rm c} = R_{\rm a}(C_{\rm a} + 2C_{\rm b})$.

IV. EXPERIMENTAL RESULTS FOR TIME DELAY, $\tau_{\rm c,exp}$

A. Calibration experiment for $\tau_{\rm c,exp}$

The time $\tau_{\rm c}$ characterizes the cable-set used in experiments and theoretically it does not depend on frequency. However, when we experimentally determine $\tau_{\rm c,exp}$, we find a frequency dependent quantity.

Let us go back on Fig.1 (section II), where the basic experiment is in fact the calibration experiment to obtain $\tau_{\rm c,exp}(f)$. First, we measured the resistor on the adaptor without the use of cables, and found a tiny but measurable imaginary part B_0, visible in Fig.1. Second, we connected the metallic resistor to the termination of the cable-set and we measured again with the impedance analyzer (see inset of Fig.1). In that case, as indicated by Eq.(20) and Eq.(25), the imaginary part of the admittance $\mathscr{I}(Y)$ is directly $G\omega\tau_{\rm c,exp}(f) + B_0$. We finally obtain $\tau_{\rm c,exp}(f)$ using ω and G, which are accurately known, and taking into account the small intrinsic susceptance B_0 of the component, as follows,

$$\tau_{\rm c,exp}(f) = (\mathscr{I}(Y) - B_0)/(2\pi f G) . \tag{27}$$

Experimental results obtained using Eq.(27) and Fig.1 are reported in Fig.5 for the cable combination combi-1 (see table I and II for characteristics of cables and their serial combinations), at temperatures of 300 K and 1.5 K, and using two metallic resistors. For 1.5 K, cables c_1 are mounted on an experimental rod and are introduced into a cryostat. Outside the cryostat, we used the same standard cables c_{00} than for the $T = 300$ K experiment. Solid horizontal lines in Fig.5 correspond to the theoretical values obtained using Eq.(25) and data of table I and II. We have used c_1 for the cable "a" connected to sample, and two cables c_{00} for the cable "b". The expected theoretical values in Fig.5 are $\tau_{\rm c}(300\,{\rm K}) = 72.8$ ns, and $\tau_{\rm c}(1.5\,{\rm K}) = 52.5$ ns (table II).

Both components give a coherent determination of

TABLE I. List of coaxial cables used in our experiments. Time delay $\tau_{\rm a}$ is calculated from Eq.20. Except mentioned, $T = 300$ K. For all cables, the characteristic impedance is $Z = 50\,\Omega$.

cable	$\rho(\Omega/m)$	length(m)	R(Ω)	C(pF)	$\tau_{\rm a}(ns)$
c_1	26.6	2.4	64	335	21.4
c_1 (1.5 K)	19	2.4	46	335	15.4
c_2	2.3	2.0	4.6	201	0.9
c_2 (1.5 K)	1.1	2.0	2.2	201	0.4
c_3	2.4	3.0	7.2	300	2.3
c_4	2.1	2.0	4.2	192	0.8
c_0	0.22	1.0	0.22	100	≈ 0.02
c_{00}	0.22	2.0	0.45	200	≈ 0.1

TABLE II. Calculated delay for cables combinations (eq.25), $T = 300$ K.

combination	cables	$\tau_{\rm c}(ns)$
combi-1	$c_1 + 2\,c_{00}$	72.8
combi-2	$c_1 + 2\,c_{00}$ (1.5 K)	52.5
combi-3	$c_2 + c_{00}$	2.85
combi-4	$c_2 + c_{00}$ (1.5 K)	1.4
combi-5	$c_4 + c_3$	5.4
combi-6	$c_3 + c_0$	3.6
combi-7	$c_4 + 2\,c_0$	2.7
combi-8	c_3 twisted	2.3

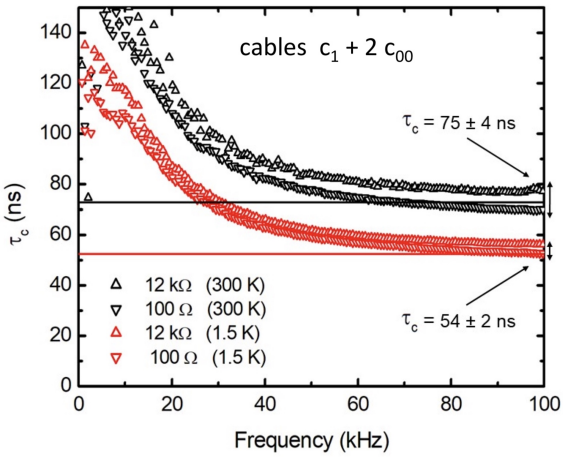

FIG. 5. Experimental delay $\tau_{\rm c}(f)$ for combination of cable $c_1 + 2\,c_{00}$. Both families of curves correspond to room temperature ($T = 300$ K) and pumped Helium temperature ($T = 1.5$ K). There were obtained using two different metallic resistors indicated in inset. Solid horizontal lines correspond to the theoretical values reported in table II.

$\tau_{c,exp}(f)$, but the experimental values correspond to the theoretical ones only above 50 kHz. Below this frequency, deviation from the expected value increases. Contrarily, at 100 kHz and for $T = 300$ K, the data dispersion is small $\Delta\tau_c(\text{exp}) = \pm 4$ ns, and the experimental values fit the theoretical ones.

The deviations of $\tau_{c,exp}$ from theoretical values at low frequencies, cannot be attributed to the cable capacitance nor to the cable resistance: we have checked that those quantities do not vary at all below 100 kHz, as expected. Moreover, the skin effect[53] does not intervene here because for our cables (conductors composed of a silver multi-strand wire) the skin depth at 100 kHz is 63 μm and comparable with the diameter of the whole wire (100 μm), but more, the skin effect increases with frequency, while the problem here appears at low frequency.

Instead, we attribute the increase of $\tau_{c,exp}$ at low frequencies, to a bad determination of small susceptances at very low frequency by our impedance analyser. The measurement accuracy is indicated on the reactance chart in Agilent handbook[54], which explicitly shows that the error exceeds 10 % when measuring $G\tau_c$ (which acts as a capacitance ≈ 0.1-1pF in our experiments) using frequency below 50 kHz. The measurement uncertainty increases even further at lower frequencies, and it might be diverging and larger than 100 % below 15kHz. By the way, the observable enhanced noise at very low frequency is also attributed to the imprecision of the impedance analyzer below 15kHz (see Refs.[6,44]), and supports the same conclusion. In fact, we show in section IV that the appropriate frequency range in our conditions is [50 kHz, 1MHz]. However, despite low frequency deviations from the model, we stress that we can still reconstruct the signal once we obtain the experimental function $\tau_{c,exp}(f)$ in the whole frequency range. This function indeed, takes into account the overall environment proper to each experiment, including cables, including any systematic error introduced by the impedance analyser itself.

The accuracy of the calibration method can be assessed by repeating the same procedure described above, employing various metallic resistors or 2DEG samples. As illustrated in Fig.5 and Fig.7, the experimental results for τ_c exhibit slight variations when different samples are used. Clearly, data dispersion determines the minimal experimental uncertainty. As shown in sections *B* and *C* below, the precision of τ_c determination using our experimental setup, is always above $\Delta\tau_c = 0.2$ ns, and can be as high as $\Delta\tau_c = 4$ ns.

B. Retrieving the true susceptance: a toy experiment

In this section, we show that the systematic error introduced by both the cables and the impedance-analyzer can be subtracted to obtain the true value of susceptance, up to some accuracy lost. We measured the admittance of three dipoles: the dipole D1 which is a test capacitance $C_{test} = 2.9 \pm 0.1$ pF; D2 is C_{test} in parallel with resistor $R_1 = 12\,\text{k}\Omega$; D3 is C_{test} in parallel with $R_2 = 24\,\text{k}\Omega$. All dipoles are thus supposed to have the same imaginary part and they are all measured at the end of the same combination of cables combi-1, as for the calibration experiment. We reported in Fig.6 the imaginary part of

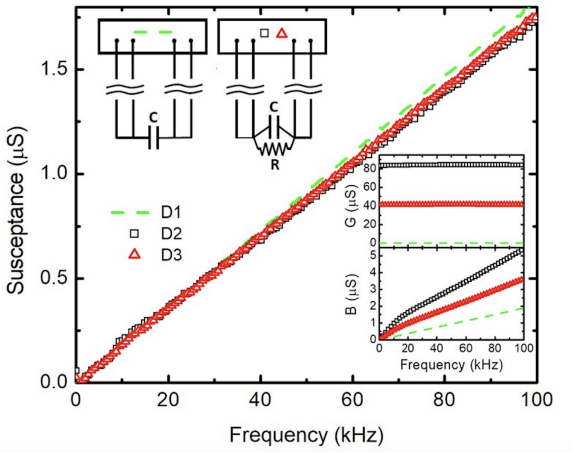

FIG. 6. Direct imaginary part of admittance versus frequency for capacitance alone (green dashed line), and imaginary part after correction for D2 and D3. All dipoles are placed at the end of combi-1. In inset, rough data of the admittance real and imaginary part for D1, D2 and D3. $T = 300$ K.

the admittance for the capacitance alone (D1), and the imaginary part of the admittance after correction for D2 and D3. In inset, we reported rough measurements of the admittance before correction.

The correction consists in applying the procedure described in section III-D, using the experimental time delay defined by Eq.(27). For this, we used $\tau_{c,exp}(f)$ shown on Fig.5 (obtained with combi-1 cables as well). We observe in inset of Fig.6 a slope break around 20 kHz in the susceptance, which is due to the artificial low frequency enhancement of $\tau_{c,exp}(f)$, and which disappears with help of the procedure. In Fig.6 indeed, we observe a satisfactory linear increase with frequency for susceptance of D2 and D3. We finally obtain $C_{test} = 2.8 \pm 0.3$ pF using D2, a result still in agreement with the constructor data $C_{test} = 2.9 \pm 0.1$ pF. Meanwhile, the uncertainty is of course increased compared to the case in which the capacitance is measured alone. The uncertainty is entirely due to bad determination of time delay $\Delta\tau_{c,exp} = \pm 4$ ns (see Fig.5), which results in $\Delta(G\tau_{c,exp}) \approx 8.10^{-5} \times 4.10^{-9} \approx 0.3$ pF.

In the present example, the experimental environment is not suitable for this measurement. Indeed, the additional phase introduced by cables, $\omega\tau_c = 4.6\ 10^{-2}$rad at 100kHz, is of same order of magnitude than the measured phase of dipole D2 at 100kHz ($\varphi_{measured} = B/S = 6.8\ 10^{-2}$rad). The real phase is $\varphi_{sample} = 2.2\ 10^{-2}$rad, and it is clear that the phase introduced by the cables adds directly to the signal phase, to give the measured phase.

Consequently, an objective, quantitative criterion can be established to determine whether the experimental context is adequate: the measurement is free from systematic errors if the phase added by the cables ($\omega\tau_c$) is significantly smaller than the measured phase of the signal at this frequency. It is therefore essential to estimate or to measure the time τ_c of the experimental system, prior to sample analysis. In general, and to be more precise, experimental constraints impose limits on

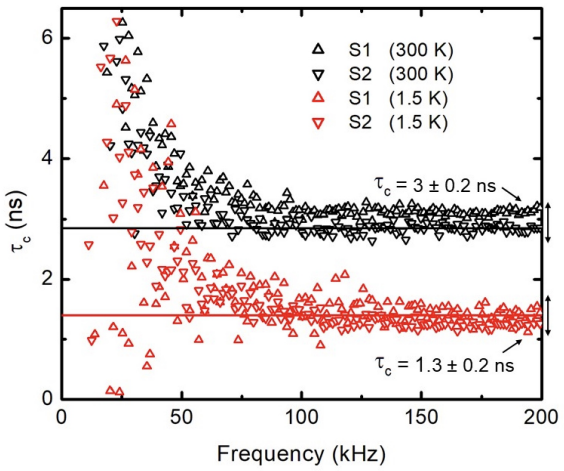

FIG. 7. Experimental delay $\tau_{c,exp}$ for combi-3 and combi-4. For each temperature, both curves have been obtained using two different samples processed on a same AlGaAs/GaAs hererojunction, whose 2D electron density is $N_s = 4.3\,10^{11}\,cm^{-2}$ and mobility is $\mu = 42\,m^2$/V.s. The sample consists in a single channel 2 mm long and 200 μm wide for S1 (400 μm for S2).

the value of τ_c, which cannot be less than 10^{-11} s (the approximate value for a 1m coaxial cable with a resistance of 0.1 Ω), and can be as large as 10^{-7} s, like in our case. Consequently, at 1 MHz, $\omega\tau_c$ ranges from 10^{-5} rad to 10^{-1} rad, a quantity to be compared to the sample phase. If these two phases are comparable, the systematic error introduced by the cables can nevertheless be deducted from measurement to find the real phase, but this operation will result in a minimal final uncertainty $\omega\Delta\tau_c$.

Clearly here, cable c_1 won't allow accurate measurement of capacitances below 1pF if there's a resistor in parallel. Less resistive cables are needed to accurately measure smaller capacitances. This is the subject of the next paragraph.

C. Characteristic time delay for low resistive cables

From now we are concerned with cables whose resistance is much less than for cable c_1, but still finite and $\geq 1\,\Omega$. Such cables bring some heat in the cryostat, however they enable more accurate measurements. Characteristics of cables and their combinations are reported in tables I and II. The characteristic time τ_c (Eq.25), contains contribution of 4 identical cable combinations, that we connect between the four sockets of impedance analyzer and the dipole under test.

Results for combi-3 are reported in Fig.7 up to 200 kHz. Experiments was carried out using a two-dimensional electron gas (2DEG) found at the interface of a AlGaAs/GaAs heterojunction. A 2DEG has indeed a vanishing imaginary part at zero magnetic field. The kinetic inductance of a 2DEG is $L_{kin} = R\tau_d$ where the diffusion time is $\tau_d \approx 1$ ps[52]. For our sample with a typical $k\Omega$ resistance, the kinetic inductance L_{kin} is in the nH range and too small to be measured here.

Measurements seem closer to the model than in Fig.5 for combi-1, because we increased the frequency range. Low frequency enhancement is attributed again to a bad measurement from the impedance analyzer at these frequencies. Besides, we notice as well a large dispersion of experimental points for low frequencies. However, the data dispersion at high frequency is small enough for an accurate determination of a 0.1 pF capacitance. We performed same experiment with same combination of cables but at pumped Helium temperature (refered as combi-4 in table II). At $T = 1.5$ K and 100 kHz, we measure $\tau_{c,exp} = 1.3 \pm 0.2$ ns, this value is lower than for room temperature, due to the decrease of the cable resistance.

In Fig.8 we reported experimental and theoretical values for combinations combi-5, combi-6 and combi-8. We obtain again a good agreement between experimental and theoretical values for τ_c, at high frequencies. It is remarkable that all combinations of cables exhibit the same behavior for $\tau_{c,exp}$, which claims again for a systematic imperfect measurement at low frequencies, due to the impedance analyser itself.

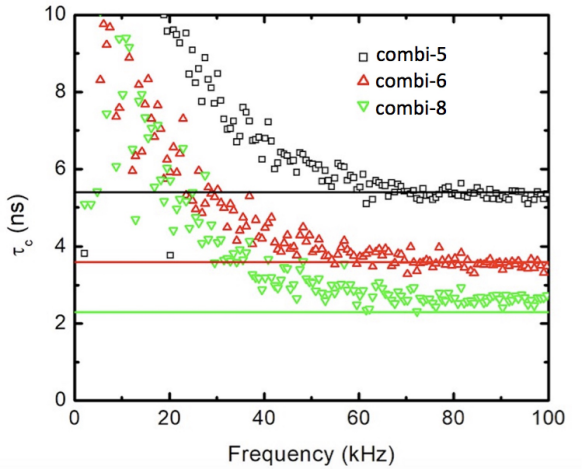

FIG. 8. Delay $\tau_{c,exp}$ for combi-5, combi-6 and combi-8 defined in Table II. Solid horizontal lines correspond to the expected theoretical values. $T = 300$ K.

D. Influence of cables relative position

The uncertainty in the determination of $\tau_{c,exp}$ results from three main difficulties. The first is the unavoidable presence of stray capacitances (of sample holder for instance) or parasitic inductances (of wire-bonding when we used 2DEG), which introduce an error proper to each experimental situation. This un-determination is observable in Fig.5 and Fig.7 through the dispersion of curves obtained in same conditions with different samples, while they should be superimposed. The second difficulty is due to deviations at low frequencies caused by the impedance analyser itself. The third difficulty lies in the control of relative position of all cables. We reported in Fig.9, results of three experiments made with same resistor and same set of cables (combi-8). Relative position of

cables was modified between each experiment and is schematized in inset: twisted cables with no space between each other, cables parallel but spaced out, and widely spaced out. We observe first, that the results obtained for twisted cables are the closest to the theoretical model. Second, it is clear that the more the space between cables, the more the results deviate from expected behavior. For all results presented in this paper (except mentioned, as in this part) we have used twisted cables. In an experimental campaign indeed, unfixed cables would make the time delay to vary from one experiment to another. Therefore, cables should always be twisted or at least gathered and attached together in order to suppress ground loops: when cables are twisted, small magnetic fields induced by current flowing through cables compensate, while large open loops cannot guarantee a precise measurement free of interferences[51]. Of course, very high-quality rigid coaxial cables should perfectly shield electric fields and avoid interferences; but generally speaking, what is often used in laboratories are standard cables and RF connectors.

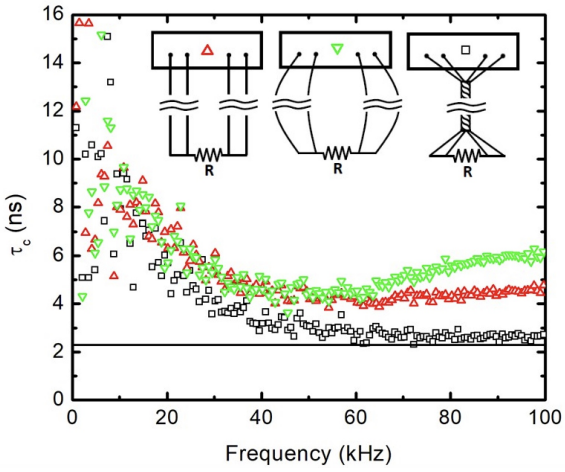

FIG. 9. Delay $\tau_{c,exp}$ for combination of cables combi-8, and three different relative arrangement for cables schematized in inset. Full horizontal line corresponds to expected theoretical value (see Table II). The twisted cables give the lower time delay and best result compared to the model. $T = 300\,\mathrm{K}$.

E. behavior at higher frequency

The characteristic $\tau_{c,exp}(f)$ is the identity card of the cable set. It allows to define the range of frequencies for more accurate measurements. In Fig.10, we present ID cards for combi-6 and combi-7 (see table II) and frequencies up to 1 MHz. In combi-6 cables are twisted while they were not in combi-7. The deviation from expected value in the case of combi-7 is attributed to open configuration of cables, which persist until 1 MHz and probably more. Contrarily, measurements using combi-6 (twisted cables) are fully conform to the theory above 50kHz. Thus, the appropriate frequency range in our technical environment is [50kHz, 1MHz]. Each set of cables should be characterized in its own, and used in a definite range of frequencies for which measurements are accurate.

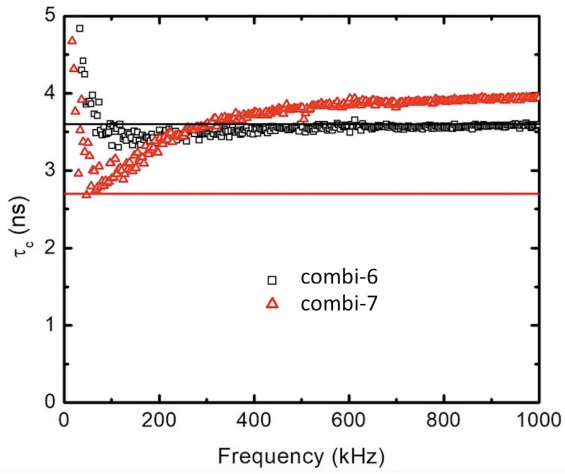

FIG. 10. Using a larger scale for frequency, we highlight differences between cables sets. $\tau_{c,exp}$ is stable, constant and close to the expected value for combi-6 (twisted cables), while it is not for combi-7 due to an open configuration of cables as in Fig.9. $T = 300\,\mathrm{K}$.

F. Magnetic field has no effect on cables behavior

We have plotted in Fig.11 values of $\tau_{c,exp}$ for combi-4 obtained using a $12\,\mathrm{k}\Omega$ metallic resistor, for several values of the magnetic field. All curves overlap completely. This allow to define $\tau_{c,exp}$ properly when working with magnetic field. As expected, coaxial cables electrical properties are not sensitive to magnetic field and thus, effect of magnetic field on sample may be distinguished easily.

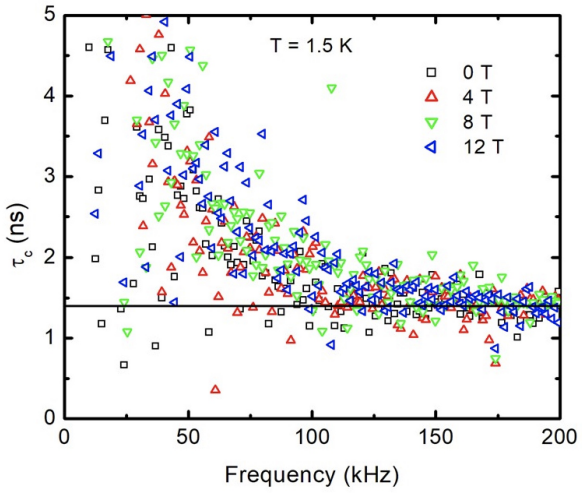

FIG. 11. $\tau_{c,exp}$ for combination of cables combi-4, using a $12\,k\Omega$ resistor and for several values of the magnetic field. Magnetic field has no effect on the electrical properties of cables. $T = 1.5\,\mathrm{K}$.

V. SUMMARY

We have exhibited and analyzed the role of coaxial cables resistance in an admittance measurement at low frequency. We obtain theoretical expressions for the measured quantities in the whole frequency range, not limited to AQSR. At low frequency, the lead resistance introduces a phase shift characterized by a time delay τ_c which depends on total resistance and total capacitance of cables. To obtain the true admittance phase, the time delay must be measured within the working frequency range (calibration experiment) and the phase shift $\omega\tau_c$ subtracted from the rough data.
Although we have been concerned here with impedance, our results extend to any a.c. electrical measurements in which the problem is to determine precisely the imaginary part. We have shown that It is essential to estimate or to measure the phase shift $\omega\tau_c$ prior to sample analysis, and compare it to the measured phase. If those two phases are comparable, the phase shift introduced by the cables should be deducted.

ACKNOWLEDGEMENTS

We warmly thank B. Reulet (Sherbrooke University, Quebec, Canada) for lightening discussions and useful suggestions at early stage of this work. This work has been partly supported by the Vicerrectoría de Investigaciones of Universidad Militar Nueva Granada, Bogota, Colombia (project INV-CIAS-2939).

APPENDIX

Measuring a potential $V_1 e^{j\omega t}$ using a series combination of two coaxial cables

We reconsider previous calculations for a measurement involving two coaxial cables in series: cable "a" on the sample side, and cable "b" on the voltmeter side, see Fig.12. The continuity relations for current and potential impose

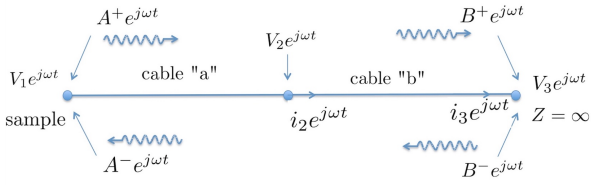

FIG. 12. Two coaxial cables in series: "a" connected to the sample side and "b" connected to measuring instruments. A^+ and A^- (resp. B^+ and B^-) are the complex amplitudes at left (resp. right) end.

$$
\begin{aligned}
i_2 &= \frac{B^+e^{-\gamma_b} - B^-e^{-\gamma_b}}{Z_b} = \frac{A^+e^{-\gamma_a} - A^-e^{\gamma_a}}{Z_a},\\
i_3 &= \frac{B^+ - B^-}{Z_b} = 0,\\
V_1 &= A^+ + A^-,\\
V_2 &= B^+e^{\gamma_b} + B^-e^{-\gamma_b} = A^+e^{-\gamma_a} + A^-e^{-\gamma_a},\\
V_3 &= B^+ + B^-.
\end{aligned}
$$

Using $B^+ = B^-$ from above, and setting $\alpha = Z_a/Z_b$, we get

$$
\begin{aligned}
A^+e^{-\gamma_a} &= B^+(\cosh(\gamma_b) + \alpha\sinh(\gamma_b)),\\
A^-e^{\gamma_a} &= B^+(\cosh(\gamma_b) - \alpha\sinh(\gamma_b)).
\end{aligned}
$$

The relation between voltages V_1 and V_3 is finally:

$$V_1 = V_3(\cosh(\gamma_a)\cosh(\gamma_b) + \alpha\sinh(\gamma_a)\sinh(\gamma_b)) \ . \qquad (A.1)$$

Measuring a current $i_1 e^{j\omega t}$ using two coaxial cables

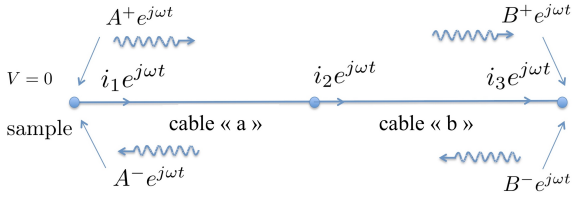

FIG. 13. $V = 0$ is imposed at left end of the coaxial cable by the a.c. bridge. Measurement of current i_1 gives i_3 at right end of cable.

Writing the three continuity relations for current and potential in Fig.13, gives the relation between i_1 and i_3:

$$i_3 = i_1(\cosh(\gamma_a)\cosh(\gamma_b) + \alpha\sinh(\gamma_a)\sinh(\gamma_b)). \qquad (A.2)$$

Measuring an impedance using 4 series of coaxial cables

In conclusion of this appendix, we obtain the phase shift which appear when measuring an admittance Y or an impedance Z with a set of 4 combinations of cable "a" in series with cable "b". If cables "a" are connected to the sample side and cables "b" are connected to impedance analyzer, the relation between experimental quantities and true values are:

$$Z_{exp} = Z/(\cosh(\gamma_a)\cosh(\gamma_b) + \alpha\sinh(\gamma_a)\sinh(\gamma_b))^2, \quad (A.3)$$

$$Y_{exp} = Y(\cosh(\gamma_a)\cosh(\gamma_b) + \alpha\sinh(\gamma_a)\sinh(\gamma_b))^2. \quad (A.4)$$

In the low frequency development ($\gamma_a, \gamma_b \ll 1$), we have

$$Y_{exp} = Y(1 + \gamma_a^2 + \gamma_b^2 + 2\alpha\gamma_a\gamma_b), \qquad (A.5)$$

which can be written as a small phase shift,

$$Y_{exp} = Ye^{j\omega\tau_c}, \qquad (A.6)$$

$$\tau_c = R_aC_a + R_bC_b + 2R_aC_b \ . \qquad (A.7)$$

[1]H.T. Wilhelm, “Impedance Bridges for the Megacycle Range,” *The Bell System Technical Journal*, 31 (1952) 999-1012.

[2]Y. Xu, X. Xie, Y. Duan, L. Wang, Z. Cheng, J. Cheng, "A review of impedance measurements of whole cells," *Biosensors and Bioelectronics* 77 (2016) 824-836.

[3]M. Rehman, B. A.J.A. Abu Izneid, M. Z. Abdullah and M.R. Arshad, "Assessment of quality of fruits using impedance spectroscopy," *Intern. Jour. of Food Sci. and Techn.* 46 (2011) 1303-1309.

[4]F. Overney, B. Jeanneret, “Impedance Bridges: from Wheatstone to Josephson," *Metrologia* 55 (2018) S119-S134.

[5]L. Callegaro, “The Metrology of Electrical Impedance at High Frequency: A Review," *Meas. Sci. Technol.* 20 (2009) 022002.

[6]K.-E. Rydler and V. Tarasso, “A Method to Determine the Phase Angle Errors of an Impedance Meter," *2004 Conference on Precision Electromagnetic Measurements*, London, UK (2004) 123-124.

[7]J. Schurr, F. J. Ahlers, G. Hein, J. Melcher, K. Pierz, F. Overney and B. M. Wood, “AC Longitudinal and Contact Resistance Measurements of Quantum Hall Devices," *Metrologia* 43 (2006) 163-173.

[8]J. Schurr, B. M. Wood and F. Overney, “Linear Frequency Dependence in AC Resistance Measurement," *IEEE Trans. Instr. and Meas.* 54 (2005) 512-515.

[9]S. W. Chua, A. Hartland and B. P. Kibble, “Measurement of the ac Quantized Hall Resistance," *IEEE Trans. Instr. and Meas.* 48 (1999) 309-313.

[10]M.E. Cage and A. Jeffery, “Intrinsic Capacitances and Inductances of Quantum Hall Effect Devices," *J. Res. Natl. Inst. Stand. Technol.*, 101 (1996) 733-744.

[11]B. Jeckelmann and B. Jeanneret, “The quantum Hall effect as an electrical resistance standard," *Rep. Prog. Phys.* 64 (2001) 1603-1655.

[12]F. J. Ahlers, B. Jeanneret, F. Overney, J. Schurr, and B. M. Wood, “Compendium for precise ac measurements of the quantum Hall resistance," *Metrologia* 46 (2009) R1-R11.

[13]F. Delahaye, B.P. Kibble and A. Zarka, "Controlling ac losses in quantum Hall effect devices," *Metrologia* 37 (2000) 659-670.

[14]B. M. Wood, A. D. Inglis and M. Côté, "Evaluation of the ac quantized Hall resistance," *IEEE Trans. Instr. and Meas.* 46 (1997) 269-272.

[15]A. Hartland, B. P. Kibble, P. J. Rodgers, and J. Bohácek, "AC Measurements of the Quantized Hall Resistance," *IEEE Trans. Instr. and Meas.* 44 (1995) 245-248.

[16]F. Delahaye, "Accurate AC Measurements of the Quantized Hall Resistance from 1 Hz to 1.6 kHz," *Metrologia* 31 (1995) 367-373.

[17]J. Schurr, J. Kucera, K. Pierz, and B. P. Kibble, “The quantum Hall impedance standard," *Metrologia* 48 (2011) 47-57.

[18]B P Kibble and J Schurr, “A novel double-shielding technique for ac quantum Hall measurement," *Metrologia* 45 (2008) L25-L27.

[19]A.T. Tran, F. Huet, K. Ngo, P. Rousseau, “Artefacts in electrochemical impedance measurement in electrolytic solutions due to the reference electrode," *Electrochimica Acta* 56 (2011) 8034-8039.

[20]B. Gustavsen, “Eliminating Measurement Cable Effects From Transformer Admittance Measurements," *IEEE Transactions on Power Delivery* 31 (2016) 1609-1617.

[21]J. Melcher, J. Schurr, F. Delahaye and A. Hartland, “Comment on "Low-frequency impedance of quantized Hall conductors"," *Phys. Rev. B* 64 (2001) 127301.

[22]W. Desrat, D.K. Maude, L.B. Rigal, M. Potemski, J.C. Portal, L. Eaves, M. Henini, Z.R. Wasilewski, A. Toropov, G. Hill and M.A. Pate, “Low-frequency impedance of quantized Hall conductors," *Phys. Rev. B* 62 (2000) 12990.

[23]C. Hernández, C. Consejo, P. Degiovanni, C. Chaubet, “Admittance of multiterminal quantum Hall conductors at kilohertz Frequencies," *J. Appl. Phys.* 115 (2014) 123710.

[24]C. Hernández and C. Chaubet, “Impedancia longitudinal de un gas bidimensional de electrones en régimen de efecto Hall cuántico," *Rev. Mex. Fis.* 55 (2009) 432-436.

[25]F. Fischer and M. Grayson, “Influence of voltmeter impedance on quantum Hall measurements," *J. Appl. Phys.* 98 (2005) 013710.

[26]J. Kucera, P. Svoboda and K. Pierz, “AC and DC Quantum Hall Measurements in GaAs-Based Devices at Temperatures Up To 4.2 K," *IEEE Trans. Instr. and Meas.* 68 (2019) 2106-2112.

[27]H Scherer, J Schurr and F J Ahlers, "Electron counting capacitance standard and quantum metrology triangle experiments at PTB," Metrologia 54 (2017) 322-338.

[28]R. D. Cutkosky, “Four-terminal-pair networks as precision admittance and impedance standards," *IEEE Trans. Commun. Electron.* 83 (1964) 19-22.

[29]B.P. Kibble, G.H. Rayner, *Coaxial ac Bridges*, Bristol, UK, Adam Hilger Ltd. (1984), paragraph 2.4.4, pp 35-36.

[30]A.J. Annunziata, D.F. Santavicca, L. Frunzio, G. Catelani, M. J Rooks, A. Frydman and Daniel E. Prober, “Tunable superconducting nanoinductors," *Nanotechnology* 21 (2010) 445202.

[31]J. Luomahaara, V. Vesterinen, L. Gronberg and J. Hassel, "Kinetic inductance magnetometer," *Nature Comm.* 5 (2014) 4872.

[32]P. K. Day, H. G. LeDuc, B. A. Mazin, A. Vayonakis, J. Zmuidzinas, "A broadband superconducting detector suitable for use in large arrays," *Nature* 425 (2003) 817-821.

[33]J. Gabelli, G. Feve, T. Kontos, J.M. Berroir, B. Placais, D.C. Glattli, B. Etienne, Y. Jin and M. Büttiker, “Relaxation Time of a Chiral Quantum R-L Circuit," *Phys. Rev. Lett.* 98 (2007) 166806.

[34]J. Gabelli, G. Feve, J-M. Berroir, B. Placais, A. Cavanna, B. Etienne, Y. Jin and D. C. Glattli, “Violation of Kirchhoff’s Laws for a Coherent RC Circuit," *Science* 313 (2006) 499-502.

[35]M. Hashisaka, H. Kamata, N. Kumada, K. Washio, R. Murata, K. Muraki, T. Fujisawa, “Distributed-element circuit model of edge magnetoplasmon transport," *Phys. Rev. B* 88 (2013) 235409.

[36]M. Hashisaka, K. Washio, H. Kamata, K. Murabi and T. Fujisawa, “Distributed electrochemical capacitance evidenced in high-frequency admittance measurements on a quantum Hall device," *Phys. Rev. B* 85 (2012) 155424.

[37]G. Sukhodub, F. Hohls and R.J. Haug, “Observation of an Interedge Magnetoplasmon Mode in a Degenerate Two-Dimensional Electron Gas," *Phys. Rev. Lett.* 93 (2004) 196801.

[38]N. Kumada, H. Kamata and T. Fujisawa, “Edge magnetoplasmon transport in gated and ungated quantum Hall systems," *Phys. Rev. B* 84 (2011) 045314.

[39]A. Delgard, B. Chenaud, D. Mailly, U. Gennser, K. Ikushima, and C.Chaubet, “Electrochemical Capacitance and Transit Time in Quantum Hall Conductors," *Physica Status Solidi B* 256 (2019) 1800548.

[40]A. Delgard, B. Chenaud, U. Gennser, A. Cavanna, D. Mailly, P. Degiovanni, and C. Chaubet, “Coulomb interactions and effective quantum inertia of charge carriers in a macroscopic conductor," *Phys. Rev. B* 104 (2021) L121301.

[41]F. Rucker and C. Pfleiderer, "Compact susceptometer for studies under transverse field geometries at very low temperatures," *Rev. Sci. Instr.* 90 (2019) 073903.

[42]K. Umeo, "Alternating current calorimeter for specific heat capacity measurements at temperatures below 10 K and pressures up to 10 GPa" *Rev. Sci. Instr.* 87 (2016) 063901.

[43]K. Buckenmaier, M. Rudolph, C. Back, T. Misztal, U. Bommerich, P. Fehling, D. Koelle, R. Kleiner, H. A. Mayer, K. Scheffler, J. Bernarding and M. Plaumann, SQUID-based detection of ultralow-field multinuclear NMR of substances hyperpolarized using signal amplification by reversible exchange, Sci Rep 7 (2017) 13431.

[44]*Agilent impedance measurement handbook*, Agilent Technologies Inc., USA (2009).

[45]B.P. Kibble, “Four terminal-pair to anything else!," *IEEE Colloquium on Interconnections from DC to microwave*, London, UK (1999), 6/1-6/6.

[46]S.A. Schelkunoff, “The Electromagnetic Theory of Coaxial Transmission Lines and Cylindrical Shields," *The Bell System Technical Journal* 13 (1934), 532-579.

[47]H. Johnson and M. Graham, *High Speed Signal Propagation: Advanced Black Magic*, Upper Saddle River, NJ, USA, Prentice Hall Press, (1993).

[48]J. Schurr, C.C. Kalmbach, F. J. Ahlers, F. Hohls, M. Kruskopf, A. Muller, K. Pierz, T. Bergsten, and R. J. Hau, "Magnetocapacitance and dissipation factor of epitaxial graphene-based quantum Hall effect devices", *Phys. Rev. B* 96 (2017) 155443.

[49]S. Droscher, P. Roulleau, F. Molitor, P. Studerus, C. Stampfer, K. Ensslin, and T. Ihn, ” Quantum capacitance and density of states of graphene”, *Appl. Phys. Lett. 96* (2010) 152104.

[50]S. Awan, B. Kibble and J. Schurr, *Coaxial Electrical Circuits for Interference-Free Measurements*, London, UK, Institution of Engineering and Technology, (2011) pp. 66-68.

[51]L. Weichert, "The avoidance of electrical interference in instruments," *J.*

Phys. E. Sci. Instrum. 16 (1983) 1003-1012.
[52] P.J. Burke, I.B. Spielman, and J.P. Eisenstein, L.N. Pfeiffer, K.W. West, “High frequency conductivity of the high-mobility two-dimensional electron gas," *Applied Phys. Lett.* 76 (2000) 745-747.
[53] John David Jackson, *Classical Electrodynamics*, John Wiley and Sons, Inc.; 3rd Edition (1998)
[54] *Agilent 4294A Precision Impedance Analyzer - Data Sheet*, USA, Agilent Technologies Inc.(2003), p. 18.